Organic Electronics 13 (2012) 351–355

Contents lists available at SciVerse ScienceDirect

Organic Electronics

journal homepage: www.elsevier.com/locate/orgel

Synthesis of an aromatic amine derivative with novel double spirobifluorene core and its application as a hole transport material

Yong Joo Cho, Oh Young Kim, Jun Yeob Lee *

Department of Polymer Science and Engineering, Dankook University, Jukjeon-dong, Suji-gu, Yongin-si, Gyeonggi-do 448-701, Republic of Korea

ARTICLE INFO

Article history:
Received 18 August 2011
Received in revised form 25 October 2011
Accepted 22 November 2011
Available online 14 December 2011

Keywords:
Double spirobifluorene core
Hole transport material
High efficiency
High glass transition temperature

ABSTRACT

A synthetic method to prepare a novel double spirobifluorene core structure was developed and a hole transport type exciton blocking material with the double spirobifluorene core was synthesized. A two step ring closing method was used to synthesize the double spirobifluorene core. The double spirobifluorene core based hole transport material showed high glass transition temperature due to rigid structure, and high quantum efficiency in green phosphorescent organic light emitting diodes because of efficient hole injection and triplet exciton blocking properties.

1. Introduction

Organic light-emitting diodes (OLEDs) have been developed for more than 20 years and are being used in display and lighting applications. Various organic emitters and charge transport materials were synthesized for OLED applications and one of the well-known core structures is spirobifluorene. The spirobifluorene core has been widely used due to the merits of thermal stability, morphological stability, chemical stability, chemical versatility and high triplet energy [1–10].

As the spirobifluorene moiety was effective as the core structure of hole transport materials and emitters, many derivatives of the spirobifluorene were synthesized [11–17]. Among the various spirobifluorene compounds, dispirobifluorene based compounds were better than spirofluorene in terms of light-emitting efficiency, thermal and morphological stability [18–22]. Dispirofluorene–indenofluorene based compounds were synthesized as the double spiro type compounds [18–22]. Other than these, several dispiro-fused fluorene compounds were reported [23,24]. However, further development of new double spirobifluorene based compounds is required.

In this work, a new core structure with a double spirobifluorene moiety was developed as a thermally stable core and the synthetic procedure to prepare the double spirobifluorene structure was studied. It was demonstrated that two step ring closing procedure can be used to synthesize the double spirobifluorene core. In addition, the application of the new double spirobifluorene core based compound as the hole transport material for phosphorescent organic light emitting diodes (PHOLEDs) was investigated.

2. Experimental

2.1. General information

1,2-Dibromobenzene, *n*-butyllithium (*n*-BuLi), sodium-*t*-butoxide, palladium(II)acetate, diphenylamine and chlorodiphenylphosphine (Aldrich Chem. Co.) were used without further purification. Hydrogen peroxide (Duksan Sci. Co.) and 2,7-dibromofluorenone (P&H Co.) were used as received. Tetrahydrofuran (THF) was distilled over sodium and calcium hydride.

* Corresponding author. Tel./fax: +82 31 8005 3585.
E-mail address: leej17@dankook.ac.kr (J.Y. Lee).

1566-1199/$ - see front matter © 2011 Elsevier B.V. All rights reserved.
doi:10.1016/j.orgel.2011.11.028

The ^{1}H and ^{13}C nuclear magnetic resonance (NMR) spectra were recorded on a Varian 200 (200 MHz) spectrometer. The photoluminescence (PL) spectra were recorded on a fluorescence spectrophotometer (HITACHI, F-7000) and the ultraviolet–visible (UV–Vis) spectra were obtained using UV–Vis spectrophotometer (Shimadzu, UV-2501PC). Samples were dissolved in THF at a concentration of 1.0×10^{-4} M. The differential scanning calorimetry (DSC) measurements were performed on a Mettler DSC 822 under nitrogen at a heating rate of 10 °C/min. The mass spectrometry (MS) was performed using a JEOL, JMS-AX505WA spectrometer in fast atom bombardment mode. Cyclic voltametry (CV) measurement of organic material was carried out in acetonitrile solution with tetrabutylammonium perchlorate at 0.1 M concentration. Ferrocene was used as the internal standard material. Elemental analysis of the materials was carried out using EA1110 (CE instrument).

2.2. Synthesis

2.2.1. 2′,7′-Dibromo-spiro(cyclopenta[def]fluorene-1,5,9′9″-bifluorene)

4-Bromo-9,9′-spirobi[fluorene] (5.70 g, 14.40 mmol) was dissolved in anhydrous THF (76 mL) under ambient atmosphere. The reaction flask was cooled to −78 °C and *n*-BuLi (2.5 M in hexane, 7.49 mL) was added dropwise slowly. Stirring was continued for 2 h at −78 °C, followed by addition of a solution of 2,7-dibromo-fluorenone (6.33 g, 18.70 mmol) in anhydrous THF (123 mL) under nitrogen atmosphere. The resulting mixture was gradually warmed to ambient temperature and quenched by adding saturated, aqueous sodium bicarbonate (200 mL). The mixture was extracted with dichloromethane. The combined organic layers were dried over magnesium sulfate, filtered, and evaporated under reduced pressure. A yellow powdery product was obtained. The crude residue was placed in another two-neck flask (250 mL) and dissolved in acetic acid (150 mL). A catalytic amount of sulfuric acid (15 mL) was then added and the whole solution was refluxed for 12 h. After cooling to ambient temperature, purification by silica gel chromatography using dichloromethane/*n*-hexane gave a white powder.

^{1}H NMR (200 MHz, $CDCl_3$): 8.26 (d, J = 8.0 Hz, 2H), 7.87 (d, J = 7.2 Hz, 2H), 7.71∼7.54 (m, 4H), 7.39 (t, J = 7.2 Hz, 2H), 7.17 (t, J = 7.1 Hz, 2H), 6.85 (d, J = 7.4 Hz, 2H), 6.62 (d, J = 7.2 Hz, 2H), 6.50 (d, J = 7.6 Hz, 2H), 6.25 (s, 2H).

^{13}C NMR (50 MHz, $CDCl_3$): 150.1, 149.0, 141.9, 140.0, 139.5, 135.0, 131.6, 130.6, 129.4, 128.6, 127.6, 124.7, 123.8, 122.2, 121.7, 121.3, 120.8, 119.8, 65.9, 50.0. MS (FAB) m/z 637 [$(M+H)^+$]. Anal. Calcd for $C_{38}H_{20}Br_2$: C, 71.72; H, 3.17 Found: C, 69.94; H, 3.31.

2.2.2. N,N,N′,N′-Tetraphenyl-spiro(cyclopenta[def]fluorene-1,5,9′,9″-bifluorene)-2′,7′-diamine (DSPN)

2′,7′-Dibromo-spiro(cyclopenta[def]fluorene-1,5,9′,9″-bi fluorene) (1.00 g, 15.71 mmol) diphenylamine (0.66 g, 39.20 mmol) and palladium acetate (0.02 g, 0.94 mmol) were dissolved in anhydrous toluene under a nitrogen atmosphere. To the reaction mixture was added a solution of tri-*t*-butylphosphine (1 M, 0.31 g, 15.71 mmol) and sodium-*t*-butoxide (0.37 g, 39.20 mmol) dropwise slowly. The reaction mixture was stirred for 12 h at 100 °C. The mixture were diluted with dichloromethane and washed with distilled water (50 mL) three times. The organic layer was dried over anhydrous magnesium sulfate and evaporated in vacuo to give the crude product, which was purified by column chromatography using *n*-hexane. The final yellowish powdery product was obtained in 75% yield.

^{1}H NMR (200 MHz, $CDCl_3$): 8.05 (d, J = 8.0 Hz, 2H), 7.81 (d, J = 7.2 Hz, 4H), 7.61 (d, J = 7.4 Hz, 4H), 7.38–6.67 (m, 20H), 6.50 (d, J = 7.6 Hz, 8H), 6.06 (s, 2H).

^{13}C NMR (50 MHz, $CDCl_3$): 149.6, 149.2, 147.8, 146.7, 142.0, 141.9, 140.1, 136.9, 136.4, 135.8, 129.8, 128.8, 128.5, 127.5, 127.11, 124.9, 123.9, 123.3, 122.3, 121.3, 120.7, 119.5, 65.7, 50.9. MS (FAB) m/z 814 [$(M+H)^+$]. Anal. Calcd for $C_{62}H_{40}N_2$: C, 91.60; H, 4.96; N, 3.45. Found: C, 91.67; H, 4.90; N, 3.37.

2.3. Device fabrication

The basic device structure used to evaluate DSPN was indium tin oxide (ITO, 50 nm)/*N*,*N*′-diphenyl-*N*,*N*′-bis-[4-(phenyl-*m*-tolyl-amino)-phenyl]-biphenyl-4,4′-diamine (DNTPD, 60 nm)/*N*,*N*′-di(1-naphthyl)-*N*,*N*′-diphenylbenzidine (NPB) or DSPN (30 nm)/bis-9,9′-spirobi[fluoren-2-yl]-methanone (BSFM):tris(2-phenylpyridine) iridium ($Ir(ppy)_3$)(30 nm, 10%)/diphenylphosphine oxide-4-(triphenylsilyl)phenyl(TSPO1, 25 nm)/LiF (1 nm)/Al (100 nm). All organic materials were deposited by vacuum thermal evaporation. Devices were encapsulated with a glass lid and a CaO getter in glove box after device fabrication. Hole only device with a device structure of ITO/DNTPD/NPB or DSPN/Al was also fabricated to compare hole injection and transport properties of DSPN and NPB. Current density–voltage–luminance characteristics of the devices were measured with Keithley 2400 source measurement unit and CS1000 spectroradiometer.

3. Results and discussion

The double spirobifluorene moiety was designed as the core structure to obtain good thermal stability due to the twisted structure and rigidity of the double spirobifluorene core. A two step ring closing method was used to synthesize the double spirobifluorene core structure with two substituents at the spirobifluorene core. One spirobifluorene unit can be formed by lithiating only one bromine unit of 2,2′-dibromobiphenyl followed by reaction with fluorenone and ring closing reaction. The other bromine unit can be lithiated and reacted with 2,7-dibromofluorenone followed by ring closing reaction, yielding the double spirobifluorene structure. The two step synthetic process can be used to functionalize only one spirobifluorene of the double spirobifluorene core. The functionalized double spirobifluorene core can be used to synthesize various materials and a hole transport material, DSPN, was synthesized as the hole transport material for green PHOLEDs in this work. Synthetic scheme of the DSPN is shown in Scheme 1. The DSPN was designed as the high triplet energy hole transport material for green PHOLEDs. The

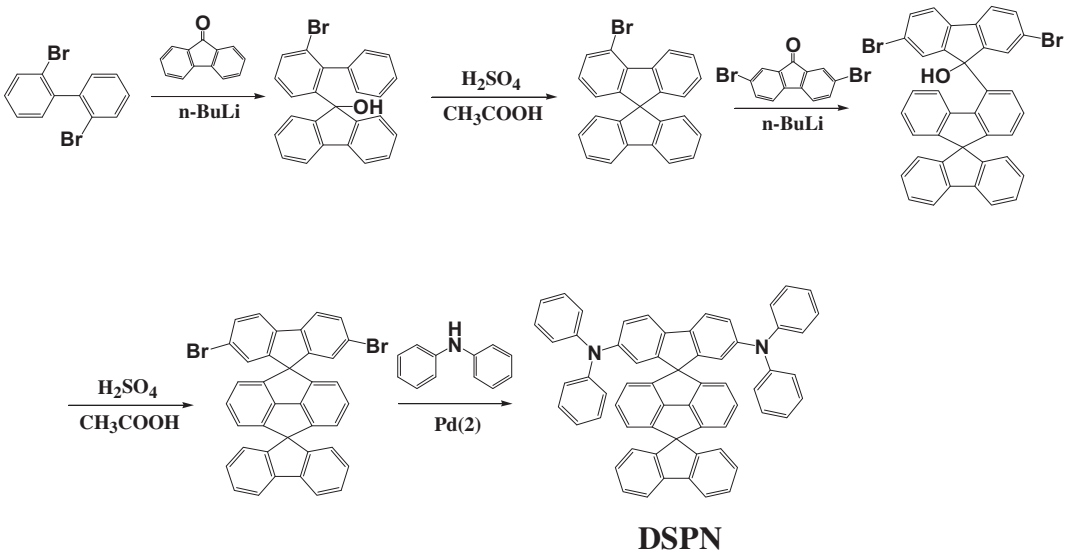

Scheme 1. Synthetic scheme of DSPN.

diphenylamine unit was introduced as the hole transport unit and was substituted at the double spirobifluorene core.

Density functional theory calculation of DSPN was carried out using a suite of Gaussian 03 program to study the orbital distribution of the DSPN. The nonlocal density functional of Becke's 3-parameters employing Lee–Yang–Parr functional with 6-31G* basis sets was used for the calculation. Fig. 1 shows the molecular simulation result of the hole transport material. The highest occupied molecular orbital (HOMO) and the lowest unoccupied molecular orbital (LUMO) of the DSPN were localized on the spirobifluorene with two diphenylamine groups. The other spirobifluorene without the attached aromatic amine group had little effect on the HOMO and LUMO. The simulated HOMO and LUMO levels of the DSPN were 4.62 and 0.90 eV, respectively.

Photophysical properties of the DSPN were analyzed using UV–Vis and PL spectrometer. UV–Vis, solution PL and low temperature PL spectra of the DSPN are shown in Fig. 2. UV–Vis absorption peaks of DSPN were observed at 309 and 373 nm. The peak at 309 nm is assigned to the π–π^* transition of the spirobifluorene unit of the double spirobifluorene core without the diphenylamine units, while the peak at 373 nm is assigned to the π–π^* transition

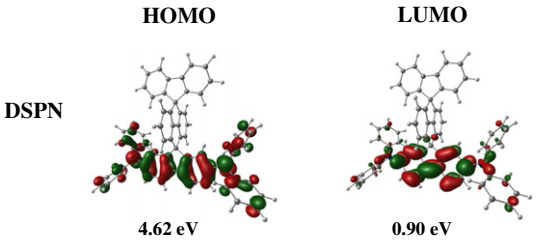

Fig. 1. HOMO and LUMO distribution of DSPN.

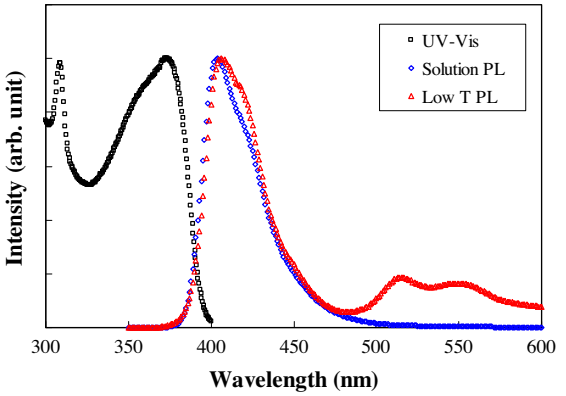

Fig. 2. UV–Vis absorption, solution PL and low temperature PL spectra of DSPN.

of the extended double spirobifluorene core through two diphenylamine units [11]. The absorption peak appeared at long wavelength due to extended conjugation. As shown in the molecular orbital simulation results, the conjugation of the DSPN is extended between two diphenylamine units, leading to the long wavelength absorption. The bandgap could be calculated from the edge of the UV–Vis absorption and was 3.12 eV. The PL emission of the DSPN was observed at 404 nm. Low temperature PL measurement was also carried out at 77 K to obtain the triplet energy of the DSPN. As the diphenylamine group extends the conjugation of the double spirobifluorene core through amine units, the triplet energy of the DSPN was 2.44 eV. The triplet energy of the DSPN was suitable for exciton blocking in green PHOLEDs.

The HOMO and LUMO of the DSPN were measured using CV and optical bandgap from UV–Vis absorption data. CV data of the DSPN is shown in Fig. 3. The HOMO

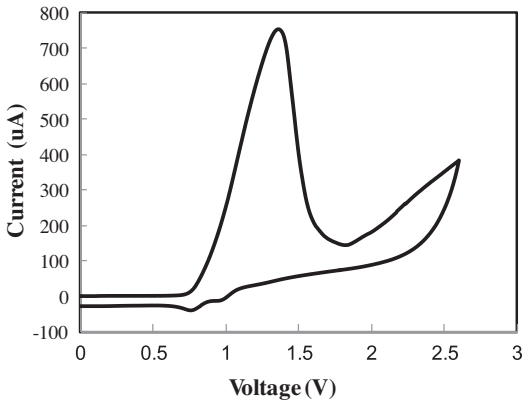

Fig. 3. CV curve of the DSPN.

and LUMO levels of the DSPN were 5.56 and 2.44 eV, respectively. The HOMO level of the DSPN was 0.06 eV deeper than that of common hole transport material like NPB (5.50 eV). The HOMO level of the DSPN is suitable for hole injection from common hole injection layer to the emitting layer and the LUMO was high enough to block electron injection from the emitting layer to the DSPN hole transport layer. In addition to the hole transport and electron blocking, the DSPN can suppress the triplet exciton quenching due to the triplet energy of 2.44 eV of DSPN compared with 2.40 eV of green phosphorescent emitter [25].

The double spirobifluorene core structure may improve the thermal properties because it has serially connected rigid spirobifluorene structure. Thermal analysis of the DSPN was carried out and high glass transition temperatures (Tg) of 152 °C was observed. Compared with common hole transport materials based on spirobiflurorene [26–28], the DSPN showed high Tg due to the rigidity of the backbone structure.

As DSPN was synthesized as the hole transport material, the hole transport properties of the DSPN were compared with those of NPB. Hole only devices DSPN and NPB were fabricated to compare the hole transport properties. Fig. 4 shows the hole only device data of DSPN and NPB. Similar hole current density was observed in the hole only devices of DSPN and NPB, indicating similar hole transport properties of DSPN and NPB. As there was 0.06 eV difference of HOMO level between DSPN and NPB, the similar hole current density implies similar hole transport properties.

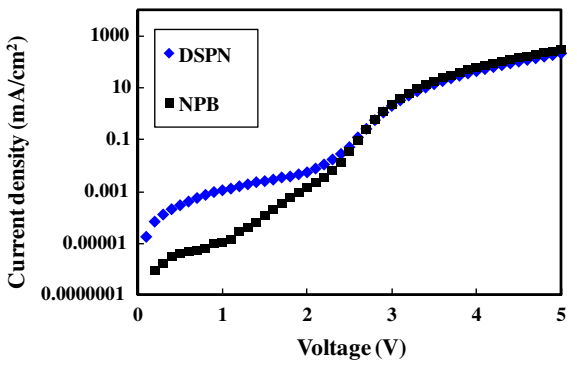

Fig. 4. Hole current density–voltage curves of DSPN and NPB hole only devices.

The DSPN has a triplet energy for exciton blocking in green PHOLEDs and was tested as the hole transport material in green PHOLEDs. Device structure and energy level diagram of the green PHOLED are shown in Fig. 5. Fig. 6 shows the current density–voltage–luminance curves of the green PHOLEDs with the DSPN as the hole transport material. The DSPN was compared with common NPB hole transport material. The current density was similar in the NPB and DSPN devices, while the luminance was high in the DSPN device. The NPB and DSPN showed similar current density due to similar energy barrier for hole injection. Although the energy barrier for hole injection from DNTPD to DSPN (0.46 eV) was slightly higher than that from DNTPD to NPB (0.40 eV), the energy barrier for hole injection from DSPN to BSFM (0.34 eV) was slightly lower than that from NPB to BSFM (0.40 eV). Therefore, the NPB and DSPN were similar in terms of energy barrier for hole injection. As shown in Fig. 4, the similar hole transport properties induced the similar current density. The luminance was rather high in the DSPN device, which is due to high recombination efficiency of DSPN device.

Quantum efficiency–luminance curves of the green PHOLEDs are shown in Fig. 7. The quantum efficiency of DSPN device was much higher than that of NPB device. Maximum quantum efficiency of NPB device was 10.4%, while that of DSPN device was 16.5%. In particular, the DSPN showed high quantum efficiency of 16.6% even at 1000 cd/m^2. The improved quantum efficiency of DSPN device is mainly due to efficient hole injection into the emitting layer and triplet exciton blocking effect. The HOMO level of the BSFM host is 5.90 eV and there is an energy barrier of 0.40 eV for hole injection from NPB to BSFM host. The high energy barrier for hole injection leads to hole accumulation at the interface between NPB and BSFM emitting layer as the BSFM host is an electron transport type host material [29,30]. Therefore, hole injection from NPB layer to BSFM emitting layer is limited by the hole accumulation. This can be confirmed in the electroluminescence (EL) spectra of the NPB device (Fig. 8). NPB emission at 450 nm was observed in the NPB device [29]. However, the hole transport layer emission disappeared in the DSPN device. The energy barrier between DSPN and BSFM was 0.34 eV, which was lower than that between NPB and BSFM. The reduced energy barrier for hole injec-

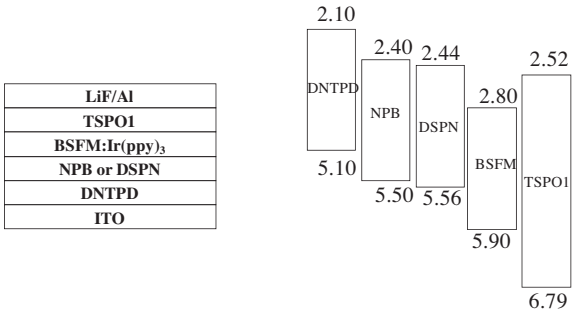

Fig. 5. Device structure and energy level diagram of DSPN device.

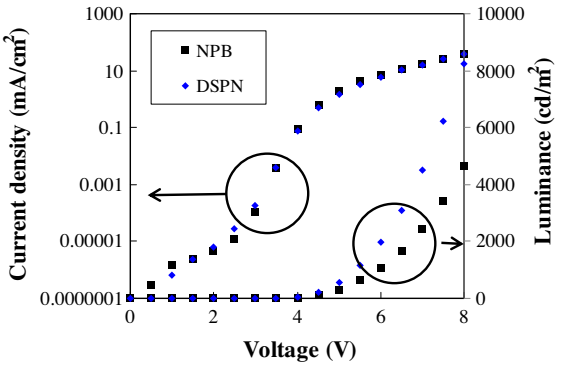

Fig. 6. Current density–voltage–luminance curves of DSPN device compared with NPB device.

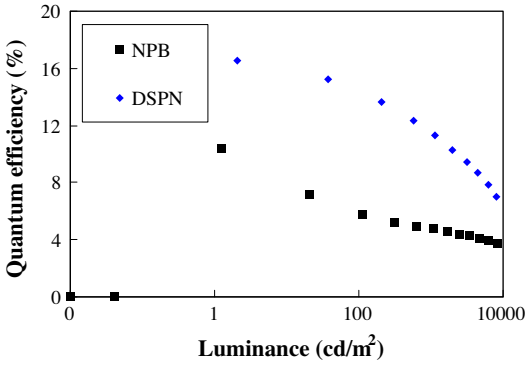

Fig. 7. Quantum efficiency–luminance curves of DSPN device compared with NPB device.

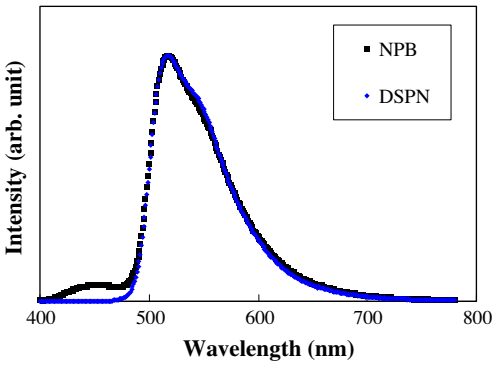

Fig. 8. Electroluminescence spectra of DSPN device compared with NPB device.

tion between BSFM host and DSPN hole transport material resulted in little hole accumulation at the interface, enhancing the quantum efficiency of green PHOLEDs. The DSPN emission was not observed in the EL spectra. Triplet exciton blocking effect of the DSPN is also critical to the high quantum efficiency of DSPN device. The triplet energy of the DSPN is 2.44 eV, which is higher than that of the $Ir(ppy)_3$ (2.40 eV). Therefore, triplet exciton quenching of $Ir(ppy)_3$ by DSPN is suppressed in DSPN devices. However, the triplet energy of NPB (2.30 eV) is lower than that of $Ir(ppy)_3$, resulting in triplet exciton quenching by NPB [30]. Therefore, the appropriate HOMO level for hole injection and high triplet energy for triplet exciton blocking improved the quantum efficiency of DSPN device.

4. Conclusions

In conclusion, a novel double spirobifluorene based hole transport material, DSPN, was effectively synthesized by two step ring closing reaction. The DSPN were efficient as thermally stable hole transport material for green PHOLEDs. Our results indicate that the double spiro type core structure is useful as the core structure for hole transport layer.

References

[1] R. Pudzich, T. Fuhrmann-Lieker, J. Salbeck, Adv. Polym. Sci. 199 (2006) 83.
[2] J. Salbeck, F. Weissoertel, J. Bauer, Macromol. Symp. 125 (1997) 121.
[3] T. Spehr, R. Pudzich, T. Fuhrmann, J. Salbeck, Org. Electron. 4 (2003) 61.
[4] J.Y. Shen, C.Y. Lee, T.H. Huang, J.T. Lin, Y.T. Tao, C.H. Chien, C. Tsai, J. Mater. Chem. 15 (2005) 2455.
[5] C. Hosokawa, H. Higashi, H. Nakamura, T. Kusumoto, Appl. Phys. Lett. 67 (1995) 3853.
[6] S.E. Jang, C.W. Joo, S.O. Jeon, K.S. Yook, J.Y. Lee, Org. Electron. 11 (2010) 1059.
[7] S.E. Jang, K.S. Yook, J.Y. Lee, Org. Electron. 11 (2010) 1154.
[8] Z. Jiang, H. Yao, Z. Zhang, C. Yang, Z. Liu, Y. Tao, J. Qin, D. Ma, Org. Lett. 11 (2009) 2607.
[9] X. Cheng, G.H. Hou, J.H. Xie, Q.L. Zhou, Org. Lett. 14 (2004) 2381.
[10] T.P.I. Saragi, T. Spehr, A. Siebert, T. Fuhrmann-Lieker, J. Salbeck, Chem. Rev. 107 (2007) 1011.
[11] S.H. Lee, B.B. Jang, Z.H. Kafafi, J. Am. Chem. Soc. 127 (2005) 9071.
[12] G. Yang, Z. Su, C. Qin, J. Phys. Chem. A 110 (2006) 4817.
[13] W.J. Shen, R. Dodda, C.C. Wu, F.I. Wu, T.H. Liu, H.H. Chen, C.H. Chen, C.F. Shu, Chem. Mater. 16 (2004) 930.
[14] C.L. Chiang, M.F. Wu, D.C. Dai, Y.S. Wen, J.K. Wang, C.T. Chen, Adv. Funct. Mater. 15 (2005) 231.
[15] S. Tao, Z. Peng, X. Zhang, P. Wang, C.S. Lee, S.T. Lee, Adv. Funct. Mater. 15 (2005) 1716.
[16] Z. Jiang, Z. Liu, C. Yang, C. Zhong, J. Qin, G. Yu, Y. Liu, Adv. Funct. Mater. 19 (2009) 3987.
[17] C. Fan, Y. Chen, P. Gan, C. Yang, C. Zhong, J. Qin, D. Ma, Org. Lett. 12 (2010) 5648.
[18] D. Horhant, J.J. Liang, M. Virboul, C. Poriel, G. Alcaraz, J. Rault-Berthelot, J. Org. Lett. 8 (2006) 257.
[19] D. Thirion, C. Poriel, F. Barrire, R. Mtivier, O. Jeannin, J. Rault-Berthelot, Org. Lett. 11 (2009) 4974.
[20] T. Kowada, T. Kuwabara, K. Ohe, J. Org. Chem. 75 (2010) 906.
[21] C. Poriel, F. Barrière, D. Thirion, J. Rault-Berthelot, Chem. Eur. J. 15 (2009) 13304.
[22] C. Poriel, J.-J. Liang, J. Rault-Berthelot, F. Barrière, N. Cocherel, A.M.Z. Slawin, D. Horhant, M. Virboul, G. Alcaraz, N. Audebrand, L. Vignau, N. Huby, G. Wantz, L. Hirsch, Chem. Eur. J. 13 (2007) 10055.
[23] L.–H. Xie, J. Liang, J. Song, C.–R. Yin, W. Huang, Curr. Org. Chem. 14 (2010) 2169.
[24] D. Vak, B. Lim, S.H. Lee, D.Y. Kim, Org. Lett. 7 (2005) 4229.
[25] V. Adamovich, S.R. Cordero, P.I. Djurovich, A. Tamayo, M.E. Thompson, B. Andrade, S.R. Forrest, Org. Electron. 4 (2003) 77.
[26] Y.–L. Liao, W.–Y. Hung, T.–H. Hou, C.–Y. Lin, K.–T. Wong, Chem. Mater. 19 (2007) 6350.
[27] F. Steuber, J. Staudigel, M. Stössel, J. Simmerer, A. Winnacker, H. Spreitzer, F. Weissörtel, J. Salbeck Adv. Mater. 12 (2000) 130.
[28] T.P.I. Saragi, T. Fuhrmann-Lieker, J. Salbeck, Adv. Funct. Mater. 16 (2006) 966.
[29] S.H. Kim, J. Jang, J.Y. Lee, Appl. Phys. Lett. 90 (2007) 223505.
[30] K.S. Yook, J.Y. Lee, J. Ind. Eng. Chem. 16 (2010) 181.